Spectroscopy of the $N = Z - 2$ nucleus ^{46}Cr and mirror energy differences

P. E. Garrett,[1,2] S. M. Lenzi,[3] E. Algin,[4] D. Appelbe,[5] R. W. Bauer,[2] J. A. Becker,[2] L. A. Bernstein,[2] J. A. Cameron,[5]
M. P. Carpenter,[6] R. V. F. Janssens,[6] C. J. Lister,[6] D. Seweryniak,[6] and D. D. Warner[7]

[1]*Department of Physics, University of Guelph, Guelph, Ontario N1G 2W1, Canada*
[2]*Lawrence Livermore National Laboratory, Livermore, California 94551, USA*
[3]*Dipartimento di Fisica and INFN, Padova, Italy*
[4]*Department of Physics, Eskisehir Osmangazi University, Meselik, Eskisehir, TR-26480, Turkey*
[5]*Department of Physics and Astronomy, McMaster University, Hamilton, Ontario L8S 4M1, Canada*
[6]*Physics Division, Argonne National Laboratory, Argonne, Illinois 60439, USA*
[7]*CLRC Daresbury Laboratory, Daresbury, Warrington, WA4 4AD, United Kingdom*
(Received 5 October 2006; published 9 January 2007)

Excited states in ^{46}Cr were sought using the ^{12}C(^{36}Ar,2n) reaction. Gamma rays were detected with the Gammasphere array, and the Z value of the reaction products was determined with an ionization chamber located at the focal plane of the Fragment Mass Analyzer. In addition to the ground-state band observed up to $I^\pi = 10^+$ (tentatively 12^+), five states are proposed to belong to the 3^- band. The mirror energy differences with the analog states in ^{46}Ti present a pronounced staggering effect between the odd and even spin members that is reproduced well by shell-model calculations incorporating the different Coulomb contributions, monopole, multipole, and single-particle effects together with an isospin-nonconserving interaction that accounts for the so-called $J = 2$ anomaly. Dramatically different $E1$ decay patterns for members of the 3^- band between the ^{46}Cr and ^{46}Ti mirrors are also observed.

I. INTRODUCTION

Assuming that the nuclear force is charge symmetric, the absolute difference in binding energy between the ground states of mirror nuclei belonging to the same isospin multiplet, T should be due to Coulomb effects only, and this energy difference is referred to as the Coulomb displacement energy (CDE). Since the ground states of mirror nuclei are analog states, the energy scale can be renormalized, removing the bulk of the CDE, by examining the energies of excited levels. The mirror energy difference (MED), the difference in excitation energies for states of the same isospin T and angular momentum I, thus might be expected to vanish. That they do not is a reflection of a number of small Coulomb effects, including the spatial correlations of the valence particles in the nucleus [1] and subtle differences in the nuclear radius as a function of the angular momentum [2]. In reality, it is known that the nucleon-nucleon interaction is not charge symmetric or independent but has an isovector contribution on the order of 1% in magnitude and an isotensor contribution on the order of 2% of the strength of the isoscalar interaction [3–5]. By examining the MED of a mirror pair as a function of increasing angular momentum, insight is gained into the total isovector interaction, the bulk of which is expected to be due to Coulomb effects. This has been exploited in studies of many $T = 1/2$ mirror pairs [6–18]. However, effects from the charge-symmetry and charge-independence breaking of the nuclear interaction may be nearly as large as those induced by the Coulomb interaction [2]. Recently, it has been suggested [6–8,19] that the electromagnetic spin-orbit interaction [20], composed of both Larmor and Thomas terms, may be playing a role in the MED of states involving the promotion of a particle between two orbitals that have opposite spin-orbit couplings,

such as that for $d_{3/2}$ $(l - s)$ to $f_{7/2}$ $(l + s)$. The electromagnetic spin-orbit interaction is opposite but unequal for protons and neutrons because the Larmor term changes signs, owing to the change in sign of the magnetic moment, and the neutron has no Thomas term [20].

The study of MEDs has been intense over the past decade, in large part because of the coupling of large-scale Ge arrays such as Gammasphere, EUROBALL, and GASP to powerful auxiliary devices. This coupling has allowed access to nuclei near the $N = Z$ line, permitting the exploration of isospin pairs, most notably the $T = 1/2$ pairs. Study of even-even $T = 1$ mirror pairs has been more limited, owing to the increased difficulty in populating the required $N = Z - 2$ nuclei. In fact, until quite recently, the highest spin in which the $T = 1$ states were observed in an even-even mirror pair was spin 6 in the $A = 42$ system [21]. Knowledge of even-even mirror pairs improved with the observation of the ground-state bands in ^{46}Cr [22] and ^{50}Fe [1], up to spin 10^+ (tentatively 12^+) and 11^+, respectively. The isovector MEDs were extracted and compared to large-scale shell-model calculations [1,22] that reproduced reasonably well the experimental data, and the contributions from both the one-body and two-body interactions, in addition to the charge-symmetry-breaking contribution from the nucleon-nucleon force, were highlighted [1,22]. Work [1,2] on the mass 50 mirror pair explored the contributing mechanisms to the MED, confirming that they are sensitive to spatial overlaps of the proton wave functions. The triplet energy difference (TED), which highlights the role of the isotensor interaction and is related to the charge independence, was extracted as a function of angular momentum in Ref. [22]. The TED was reproduced well by the shell-model calculations for both the mass 46 and 50, $T = 1$ triplets [2,22]. In the present work, levels not

TABLE I. Level scheme for ^{46}Cr determined from the ^{12}C(^{36}Ar, $2n$) reaction at 105 MeV. I_γ represents the relative γ-ray intensity, normalized to 100 for the 892.5-keV transition. Uncertainties quoted for the γ-ray energies include an estimated 0.5 keV systematic uncertainty.

E_i	$J_i^\pi \to J_f^\pi$	E_γ	I_γ
892.5(5)	$2^+ \to 0^+$	892.5(5)	100.0(10)
1987.7(7)	$4^+ \to 2^+$	1095.2(5)	61(4)
3196.9(8)	$(3^-) \to 2^+$	2304.6(7)	11.1(14)
3227.5(8)	$6^+ \to 4^+$	1239.9(5)	23.7(16)
3297(3)	$\to 2^+$	2404(3)	2.1(10)
3494.8(9)	$\to 4^+$	1506.9(8)	3.9(6)
3594.1(9)	$(4^-) \to (3^-)$	397.4(6)	3.2(4)
3594.1(9)	$(4^-) \to 4^+$	1605.3(15)	2.4(6)
3682.7(17)	$\to 4^+$	1695.0(15)	2.3(6)
3716.2(10)	$\to (3^-)$	519.3(6)	2.5(4)
3778.6(13)	$\to (3^-)$	581.7(11)	0.5(3)
3778.6(13)	$\to 4^+$	1790(3)	1.0(6)
3987.2(9)	$(5^-) \to (4^-)$	393.0(15)	0.28(16)
3987.2(9)	$(5^-) \to$	492.3(7)	1.37(24)
3987.2(9)	$(5^-) \to 6^+$	760.3(10)	1.0(3)
3987.2(9)	$(5^-) \to (3^-)$	790.1(8)	2.3(5)
4235(3)	$\to 4^+$	2248(3)	1.6(7)
4306.0(13)	$\to (4^-)$	711.8(9)	1.1(3)
4434.9(12)	$\to (4^-)$	841.0(22)	0.5(3)
4434.9(12)	$\to 6^+$	1207.4(9)	2.3(4)
4817.9(10)	$8^+ \to 6^+$	1590.4(6)	9.3(8)
4830(3)	$(6^-) \to (4^-)$	1236(3)	1.5(5)
5117(3)	$\to$	1401(3)	0.3(3)
5346(3)	$(7^-) \to (5^-)$	1359(3)	1.7(6)
6180.0(12)	$10^+ \to 8^+$	1362.1(7)	3.0(5)
8163.0(16)	$(12^+) \to 10^+$	1983.0(10)	1.0(5)

FIG. 1. (Color online) ΔE vs E plot from events recorded with the ionization chamber placed at the focal plane of the FMA. The color scale is proportional to log(counts per channel), and the regions associated with $Z = 24$, 23, and 22 are indicated by Cr, V, and Ti, respectively. This histogram has been obtained with the 200 μg/cm^2 thick C target (see text for details).

belonging to the ground-state band in ^{46}Cr are reported. A subset of these levels are tentatively assigned to the $T = 1$, 3^- band. Accepting this assignment, we then extract the MEDs for the 3^- band and compare them to shell-model calculations. Marked differences in the decay pattern of the 3^- band heads in the $T_z = \pm 1$ nuclei are noted.

II. EXPERIMENTAL DETAILS AND RESULTS

The experiment to observe ^{46}Cr was performed at the Argonne National Laboratory using the ATLAS accelerator facility. Beams of ^{36}Ar, at an energy of 105 MeV, bombarded self-supporting foils of ^{12}C that were 200, 567, and 602 μg/cm^2 thick. The products of the reaction, with average recoil velocities ranging from 0.053 (thick target) to 0.056 (thin target) of c, were analyzed with the Fragment Mass Analyzer [23] (FMA). The FMA disperses reaction products at the focal plane according to their A/q values, where A is the atomic mass and q the charge state. Since this experiment concentrated on mass 46, specifically on ^{46}Cr, slits were used to select only one A/q value, corresponding to 46/15, for the ions reaching the focal plane. The position at the focal plane was determined from signals in multichannel plate (MCP) detectors. After passing through the MCP detectors, the recoiling ions were
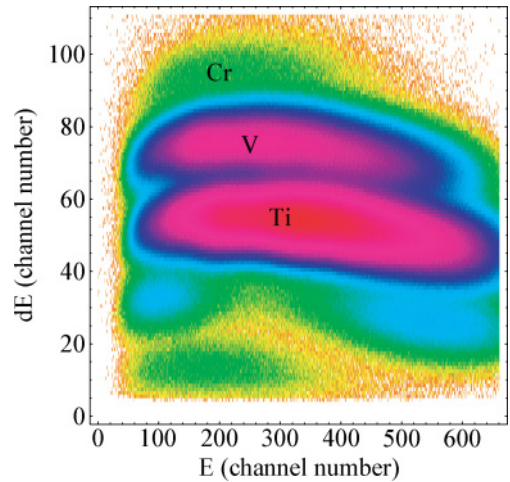
detected in an ionization chamber (IC). The signals from this counter consisted of two energy loss ΔE (ΔE_1 and ΔE_2) signals and a total energy E signal. The high recoil velocity of the mass 46 ions was sufficient to provide a high degree of Z separation in the ΔE_1 versus ΔE_2 and $\Delta E_1 + \Delta E_2$ versus E histograms. An example, obtained with the 200 μg/cm^2 target is shown in Fig. 1. The two-dimensional histogram of $\Delta E_1 + \Delta E_2$ versus E data was obtained after appropriate conditions were placed on the individual ΔE signals and on detector times relative to the beam pulse to separate the scattered beam and random events from the events of interest. The color scale is proportional to the logarithm of the number of counts in the channel, and the regions corresponding to Ti, V, and Cr ions are labeled. As can be seen, separating the reaction products according to Z is straightforward.

The γ rays from the reaction were detected with the 101 large-volume HPGe detectors of the Gammasphere array [24]. The trigger condition used for the collection of data required an event in the MCP detector and one γ event that had successfully passed the Compton-rejection veto. During playback of the data, the γ-ray events were selected by placing appropriate conditions on the various combinations of $\Delta E_1 + \Delta E_2$ versus E and ΔE_1 versus ΔE_2. Portions of the resulting γ-ray singles spectra are presented in Fig. 2 and the change in the γ-ray spectrum with the selected ion is clearly visible. The top portion of the plot is the observed spectrum with no conditions placed on the data, the spectra in panels (b), (c), and (d) correspond to the selection of Ti, V, and Cr ions, respectively. The ^{46}Ti, which results from the ^{12}C(^{36}Ar, $2p$) reaction, is the strongest of the observed reaction channels with a calculated cross section $\approx$100 mb. By using the $2^+ \to 0^+$ peak intensities as representative of the channel cross sections, the ^{46}Cr cross section can be estimated by comparing the peak areas in the respective IC-gated γ-ray singles spectra and correcting for different FMA acceptance
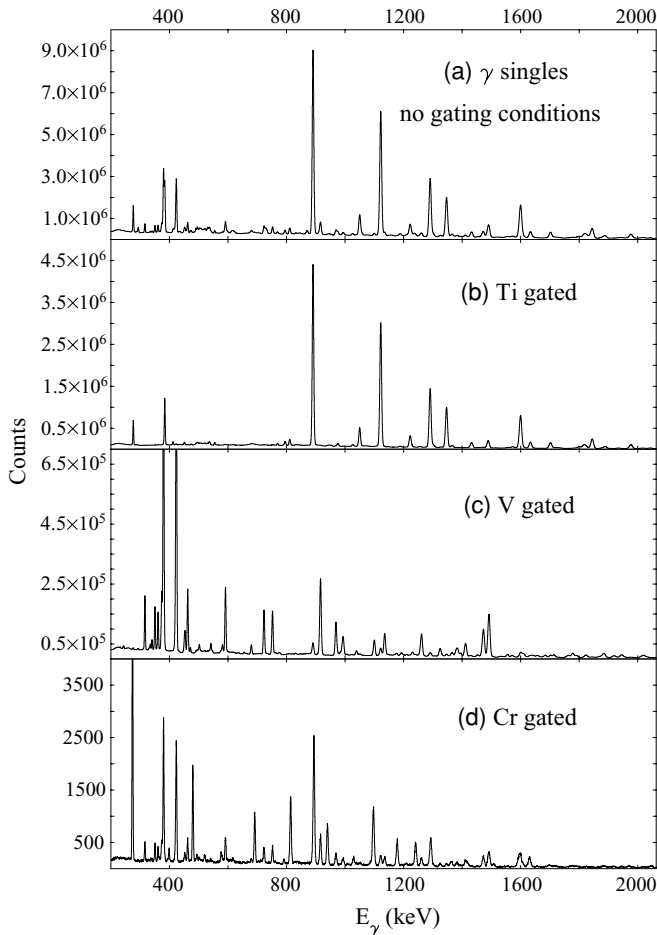
FIG. 2. Portions of the γ-ray singles spectra obtained with the ^{12}C(^{36}Ar,X) reaction with a requirement of a valid event at the FMA focal plane set to accept $A/q = 46/15$ only. The top panel (a) has no further conditions placed on the FMA data. The spectra shown in panels (b), (c), and (d) have time conditions with respect to the accelerator beam pulse set on the events and gating conditions on the IC data to select Ti, V, and Cr ions, respectively.

efficiencies and charge state distributions [25] of the recoiling Ti and Cr ions. By using this procedure, the ^{46}Cr cross section is estimated to be approximately 15 μb. The use of the FMA data was vital in extracting clean Cr γ-ray data; the ratio of the ^{46}Ti $2^+ \rightarrow 0^+$ intensity in each of the Ti, V, and Cr gated spectra was 100:1.4:0.0059.

The γ-ray singles spectrum after applying the selection on the Cr ions is presented in Fig. 3. The mass 46 Ti and V contributions to this spectrum have been subtracted, leaving only the Cr lines. Of note are the number of lines attributed to ^{49}Cr; these arise from ^{16}O(^{36}Ar,$2pn$)^{49}Cr reactions from oxygen contamination on the ^{12}C targets, the $2pn$-exit channel being one of the largest. The γ rays labeled with their energies are assigned to ^{46}Cr. Figure 4 displays portions of selected γ-ray coincidence spectra that were used to establish the level scheme presented in Fig. 5 and Table I.

The yrast band in Fig. 5 was established previously [22] up to spin 10^+ through the use of $\gamma\gamma$ coincidence relations, with a 12^+ level suggested based on the observation of a 1983-keV γ ray in the singles spectrum that matches closely in energy
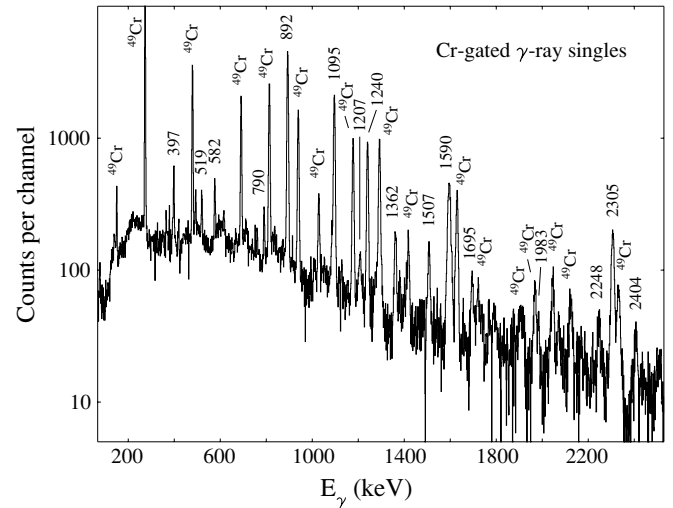

FIG. 3. Portion of the γ-ray singles spectrum created by placing conditions on events in the channel-plate detectors and the ionization chamber located on the focal plane of the FMA. The conditions used were meant to select the $Z = 24$ recoil products. Contributions from the ^{46}Ti and ^{46}V channels, created by gating on the $Z = 22$ and $Z = 23$ reaction products, have been subtracted. The peaks labeled as due to ^{49}Cr arise from (^{36}Ar, $2pn$) reactions on ^{16}O contamination on the carbon target. The peaks labeled with their energies in keV are assigned to ^{46}Cr.

the $12^+ \rightarrow 10^+$ transition in ^{46}Ti. Further work has not been able to make a firm assignment for the 12^+ level, and thus it remains tentative. Angular distributions of the transitions assigned to the yrast band, an example of which (1240-keV) is given in Fig. 6, are consistent with a stretched quadrupole character.

The strongest nonyrast transition is the 2305-keV γ ray. Coincidence relations indicate that it feeds into the 892-keV 2^+ state, establishing a level at 3197 keV. This energy matches very well the expected energy of the 3^- bandhead, which is at 3058 keV in ^{46}Ti. The 2305-keV angular distribution (Fig. 6) is consistent with that of a dipole, and thus the 3197-keV level is suggested to be the bandhead of the 3^- band. Coincidences with the 2305-keV γ ray, seen in Fig. 4, indicate a number of low-energy transitions, forming the band structure shown in Fig. 5. Angular distributions of the 397- and 790-keV γ rays are consistent with their suggested placement as $4^- \rightarrow 3^-$ and $5^- \rightarrow 3^-$ transitions, respectively.

Some very weakly populated levels were observed, including what may be the first several levels of another band starting at 3716 keV. The intensities of the respective γ rays, however, were too weak to indicate the initial spin value, and the level density near 4 MeV in ^{46}Ti is sufficiently high to exclude unique quantum number assignments based on energies alone.

III. DISCUSSION

The MED and TED for the ground-state bands in the mass 46, $T = 1$ triplet were extracted earlier and analyzed [2,22] in terms of the full-fp-space shell model and will not be repeated here. Rather, the MED associated with the 3^- band
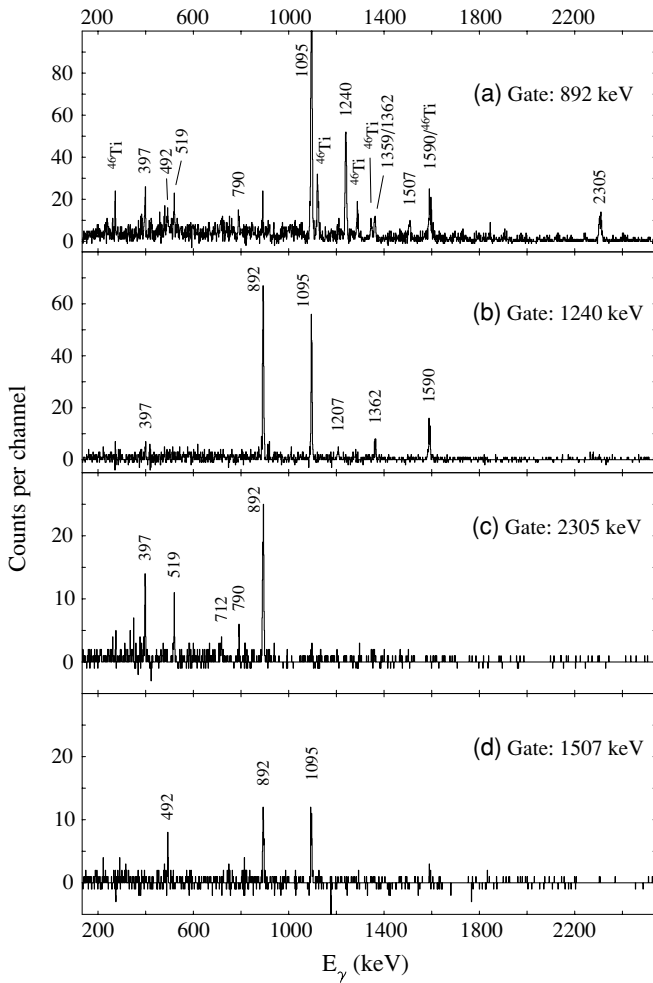
FIG. 4. Portions of the Cr-gated γ-ray coincidence spectra. The peaks are labeled with their energies in keV. The spectrum displayed in panel (a) is obtained by gating on the 892-keV $2^+ \rightarrow 0^+$ transition, in panel (b) by gating on the 1240-keV $6^+ \rightarrow 4^+$ transition, in panel (c) by gating on the 2305-keV $(3_1^+) \rightarrow 2^+$ transition, and in panel (d) by gating on the 1507-keV $(3_2^+) \rightarrow 4^+$ transition. The appearance of ^{46}Ti lines in the 892-keV gate is due to the close proximity of the 889-keV ^{46}Ti $2^+ \rightarrow 0^+$ transition.

will be investigated. Very recently [6–8,19], the study of MEDs has begun to move off the yrast line to probe excited configurations in $T = 1/2$ mirror partners. Most of these excited configurations have been of opposite parity to the yrast configuration and arise from a promotion of a $d_{3/2}$ particle into the fp shell. One of the highlights of these studies has been the observation that the electromagnetic spin-orbit term can play a substantial role in the MED [6–8,19]. This can have a large effect for states where there is a promotion of a particle between two orbitals that correspond to opposite spin-orbit couplings, such as that for $d_{3/2}$ $(l - s)$ to $f_{7/2}$ $(l + s)$. The observation of the 3^- state in ^{46}Cr allows for the extraction of the MED for an excited configuration in an even-even system for the first time. Shown in Fig. 7 are the MEDs for both the yrast and 3^- bands. The 3^- band displays a signature staggering similar to that observed in odd-A nuclei in the region (e.g. in the $A = 51$, $T = 1/2$ nuclei). Figure 8 displays

both the experimental and calculated MEDs (top panel) for the 3^- band.

The MEDs for the 3^- band were calculated by employing the ANTOINE shell-model code [26]. In the calculation for the negative-parity states, the sd core must be broken and an odd number of particles are allowed to be promoted into the fp shell. To keep the calculations tractable, only one particle was allowed to be promoted from the $d_{3/2}$ orbital into the fp shell. This calculation gives a very good description of the corresponding band in ^{46}Ti [27]. The 3^- band corresponds to the configuration where the particle is promoted into the $\frac{3}{2}^-$ [321] Nilsson orbital from the $d_{3/2}$ orbital. The calculations for the MED follow those of Zuker *et al.* [2] with the Coulomb multipole V_{CM} term that takes into account the changes in spatial correlations resulting from the angular momentum recoupling of the protons, the Coulomb monopole (radial) term V_{Cm} with a strength of $a_m = 200$ keV accounting for the change in the radii as a function of spin (essentially the change in the occupancy of the $p_{3/2}$ orbital), and an isospin-nonconserving interaction V_B that is an additional multipole term deduced from mass $A = 42$ mirror nuclei that accounts for the so-called $J = 2$ anomaly [2,15]. In addition, the single-particle Coulomb terms V_{ll} (an $l \cdot l$ term that acts only on protons) [28] and V_{ls} (the relativistic spin-orbit interaction) [20] are taken into account. Displayed in the bottom panel of Fig. 8 are the individual components of the MED, the sum of which gives the total MED that is plotted in the top panel. As can be seen, all terms give a significant contribution to the total MED, although the staggering effect is observed to be due largely to the coherent oscillations in the multipole and single-particle terms V_{CM} and $V_{ll} + V_{ls}$. The agreement of the calculation with the experimental data is impressive. The shell-model calculation indicates that wave functions for the spin 3^-, 4^-, and 6^- members of the 3^- band in ^{46}Cr (^{46}Ti) correspond to a nearly pure $d_{3/2}^{-1}(fp)^3$ neutron (proton) configuration. The 5^- and 7^- levels, in contrast, include a small component (<10% probability) with a proton (neutron) excited from the $d_{3/2}$ shell. The MED for the 3^- bandheads can be explained in terms of the single-particle effects introduced by V_{ll} and V_{ls}. In particular, the effect resulting from the electromagnetic spin-orbit interaction, which acts in an opposite way on protons than on neutrons, is the dominant one and produces a decrease of the energy gap between the $d_{3/2}$ and $f_{7/2}$ proton orbitals of ≈ 200 keV with respect to the neutron gap (calculated as in Ref. [7] using a uniformly charged sphere and free nucleon g factors). Therefore, if a neutron is excited from the $d_{3/2}$ orbit into the $f_{7/2}$ orbit in ^{46}Cr, the corresponding state will lie higher than its analog in ^{46}Ti where a proton is excited (see Fig. 7). In Fig. 8, since the data are measured relative to the 3^- bandhead, and the configuration of the states belonging to the band are similar, the MED should be expected to present very small variations. The 5^- and 7^- states appear to have a significant drop in their MED that can be related to the small components of the other type of particle excitations in the wave functions. This produces the staggering observed in the MED. The staggering would be much greater than observed except that it is counterbalanced by an opposite staggering
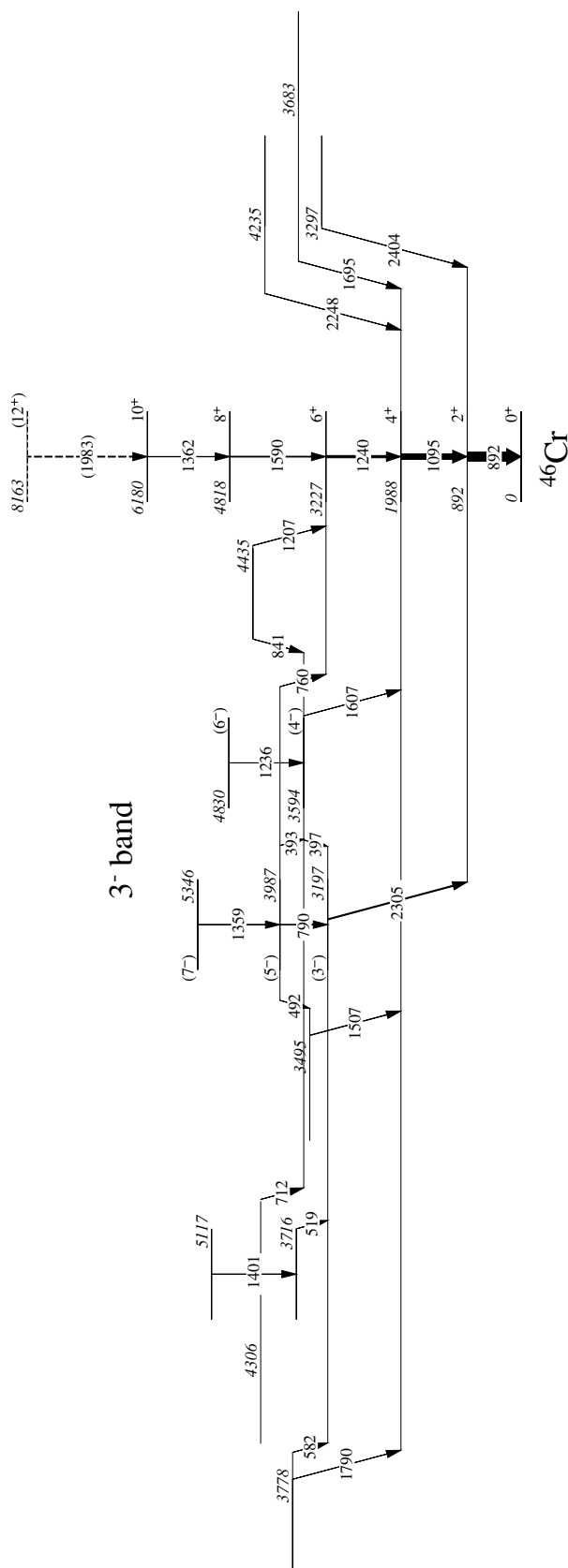
FIG. 5. Level scheme for ^{46}Cr deduced in the present work. The 1983-keV $12^+ \rightarrow 10^+$ transition in ^{46}Cr is speculative since it was observed in the $Z = 24$ gated γ-ray singles data only. Firm spin-parity assignment are shown without parentheses; those for the proposed 3^- band are consistent with the 3^- band in ^{46}Ti and angular distributions of the transitions.
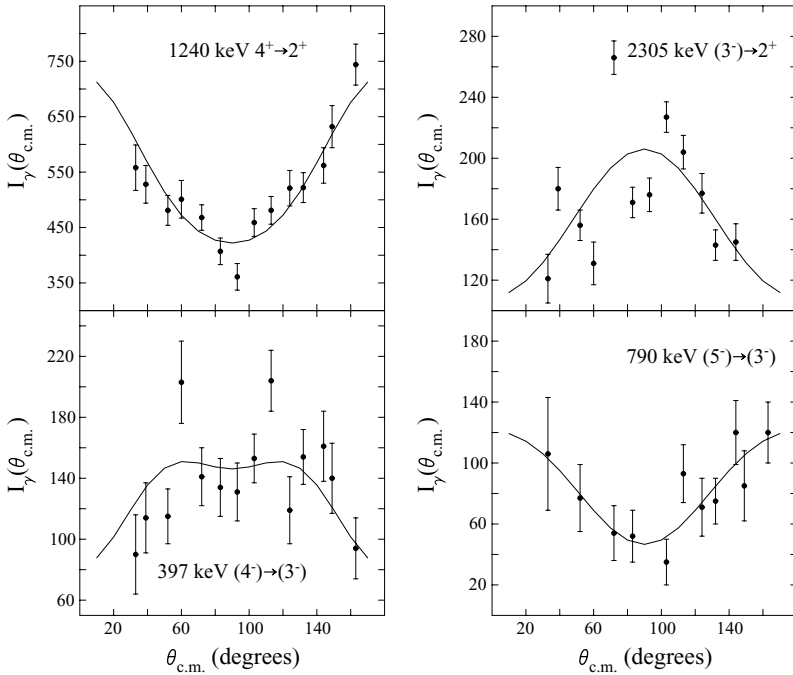
FIG. 6. Angular distributions for selected transitions in ^{46}Cr. The data were obtained by sorting the γ-ray events, gated on the Cr-ion conditions from the FMA data, according to their angle with respect to the beam direction. Corrections from the detection efficiency of the various Gammasphere rings were taken into account, as well as the laboratory-to-c.m. frame transformation.

in the monopole term caused by a smaller component of the wave functions in the $p_{3/2}$ orbital (i.e., a decreased radius) for the 5^- and 7^- states. The role of the isospin-nonconserving *nuclear* interaction is of the same order of importance as the Coulomb terms. This confirms that the role of this interaction is fundamental to reproduce the MED data, not only for yrast natural-parity states but also for the excited structures in all the hitherto measured MEDs in the $f_{7/2}$ shell. Only by considering all terms does the trend and magnitude reproduce the data.

The reduced transition rates for $E1$ decays involving analog initial and final states should be identical since only an isovector matrix element contributes and, once squared, the T_z dependence is removed [29]. This selection rule appears to be violated, however, since substantial differences have been observed in the relative decay intensities of $E1$ transitions from excited configurations to the ground-state bands in some mirror pairs. In ^{35}Ar [7], the $E1\, 7/2^- \rightarrow 5/2^+$ transition

dominates over the $7/2^- \rightarrow 3/2^+\, M2$ transition, whereas in ^{35}Cl, the $M2$ transition clearly dominates. In the mass 31 case [6], the $7/2^- \rightarrow 5/2_2^+ \gamma$ ray is comparable in strength
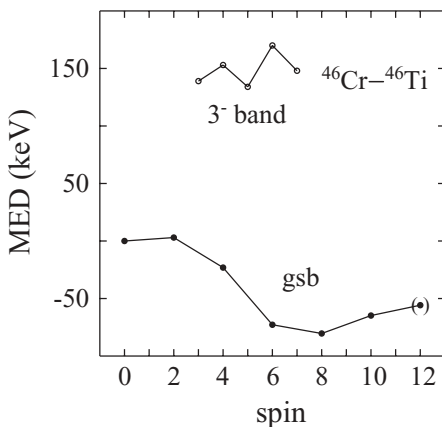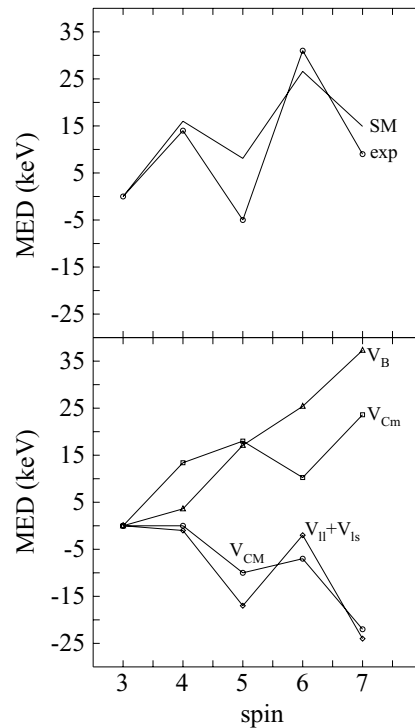

FIG. 8. Mirror energy differences, relative to the bandhead, for the 3^- band in the mirror pair ^{46}Cr and ^{46}Ti. The top panel displays both the experimental (exp) and calculated (SM) MED, whereas the bottom panel shows the individual contributions to the shell-model MED, where V_{CM} is the Coulomb multipole, V_{Cm} is the Coulomb monopole, V_B is an isospin-nonconserving interaction, and $V_{ll} + V_{ls}$ is the single-particle $l \cdot l$ and electromagnetic spin-orbit interaction.

FIG. 7. Mirror energy differences for the ground state and 3^- bands in the mirror pair ^{46}Cr and ^{46}Ti.
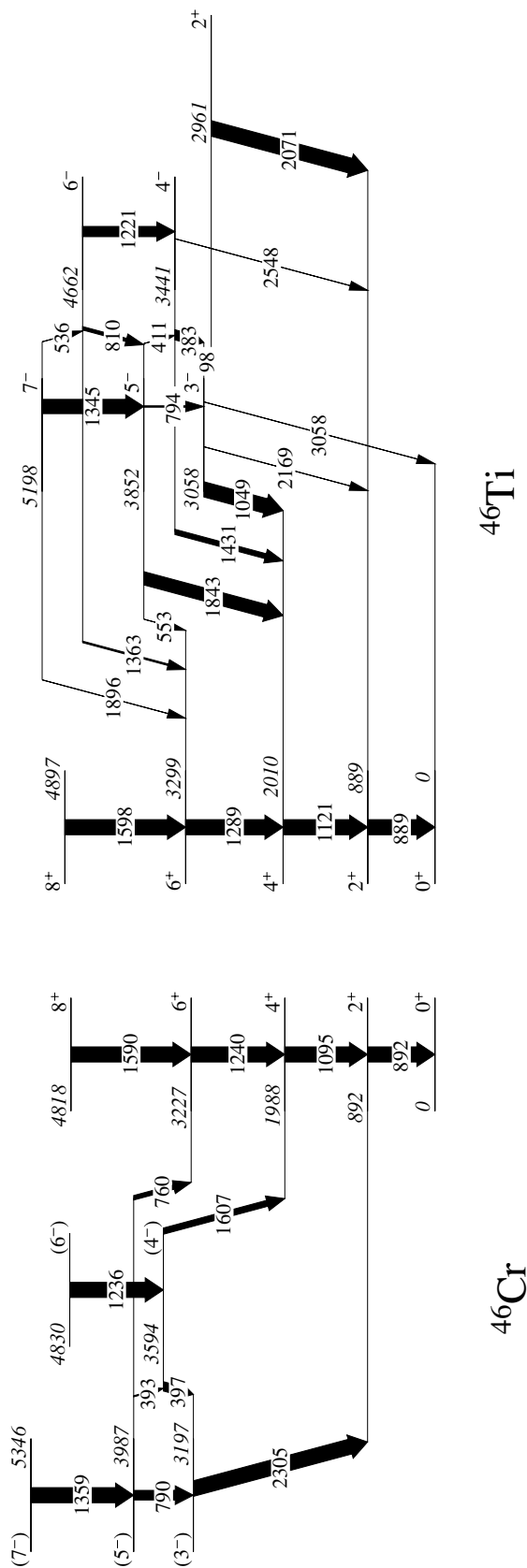
FIG. 9. Portions of the ^{46}Ti and ^{46}Cr level scheme displaying the decay of the 3^- bands. The widths of the arrows are proportional to the observed level branching ratios.

to the $7/2^- \to 5/2_1^+$ transition in ^{31}P, whereas in ^{31}S, the $7/2^- \to 5/2_1^+$ transition is essentially absent. The most recent example of different $E1$ decay intensities has been observed in the mass 45, $T = 1/2$ mirror pair [8]; in ^{45}V the $5/2_1^+$ level decays strongly to both the $3/2_1^-$ and $5/2_1^-$ states, whereas, in ^{45}Ti, the $5/2_1^+$ level has a weak branch to the $3/2_1^-$ state and no observed branch to the $5/2_1^-$ level. In the present case, the selection rule implies that the E_γ^3 weighted $E1$ branching ratios from the 3^- band to members of the ground-state band should be identical in ^{46}Cr and ^{46}Ti. Shown in Fig. 9 are portions of the ^{46}Ti and ^{46}Cr level schemes that display the decays of the levels of the 3^- bands. The widths of the arrows are proportional to the observed branching ratio for each level. In ^{46}Ti, the dominant decay branches of the 3^- and 5^- levels proceed to the 4^+ level of the yrast band. In ^{46}Cr, the 3^- level is observed to decay to the 2^+ yrast state only, and the strongest decay branch for the 5^- level is the in-band $5^- \to 3^-$ transition followed by the $5^- \to 6^+$ branch. The 4^- levels in both nuclei have comparable in-band transitions and $4^- \to 4^+$ decays, and the decay of the 6^- state is similar (the 7^- level is too weakly populated for other branches to be observed). Since the decays of the 4^- and 6^- states are similar in the two nuclei, it is suggested that there may be a significant signature effect, not only in the MEDs for the 3^- band, but also in the $E1$ decay matrix elements. This may be an indication that isospin symmetry is broken by excitations out of the sd shell. It should be noted that the asymmetry in the $E1$ decays to date involves non-natural parity excitations in the sd or $f_{7/2}$ shell. It would be of great interest to extend these studies to higher mass nuclei where $E1$ decays not involving particles or holes in the sd shell could be examined.

IV. CONCLUSIONS

In summary, an experiment to observe ^{46}Cr using the ^{12}C(^{36}Ar, $2n$) reaction with Gammasphere and the FMA has been performed. By selecting events corresponding to $Z = 24$ in the data, the yrast band in ^{46}Cr has been established up to 10^+ (tentatively 12^+), and the negative-parity 3^- band is assigned based on experimental observables and the location of the analog band in ^{46}Ti. The mirror energy difference of the 3^- band in ^{46}Cr and ^{46}Ti displays a signature staggering that is reproduced remarkably well in shell-model calculations. These are the first shell-model calculations of the MED for non-natural-parity bands in the $f_{7/2}$ shell. The $E1$ decays may also display a significant difference that is dependent on signature between the 3^- band in ^{46}Cr and ^{46}Ti, suggesting a breaking of isospin symmetry in excitations out of the sd shell.

[1] S. M. Lenzi, N. Marginean, D. R. Napoli, C. A. Ur, A. P. Zuker, G. de Angelis, A. Algora, M. Axiotis, D. Bazzacco, N. Belcari, M. A. Bentley, P. G. Bizzeti, A. Bizzeti-Sona, F. Brandolini, P. von Brentano, D. Bucurescu, J. A. Cameron, C. Chandler, M. De Poli, A. Dewald, H. Eberth, E. Farnea, A. Gadea, J. Garces-Narro, W. Gelletly, H. Grawe, R. Isocrate, D. T. Joss, C. A. Kalfas, T. Klug, T. Lampman, S. Lunardi, T. Martinez, G. Martínez-Pinedo, R. Menegazzo, J. Nyberg, Zs. Podolyak, A. Poves, R. V. Ribas, C. Rossi Alvarez, B. Rubio, J. Sanchez-Solano, P. Spolaore, T. Steinhardt, O. Thelen, D. Tonev, A. Vitturi, W. von Oertzen, and M. Weiszflog, Phys. Rev. Lett. **87**, 122501 (2001).
[2] A. P. Zuker, S. M. Lenzi, G. Martínez-Pinedo, and A. Poves, Phys. Rev. Lett. **89**, 142502 (2002).
[3] E. M. Hendley, in *Isospin in Nuclear Physics*, edited by D. H. Wilkinson (North Holland, Amsterdam, 1969), p. 17.
[4] G. Q. Li and R. Machleidt, Phys. Rev. C **58**, 1393 (1998).
[5] R. Machleidt, Phys. Rev. C **63**, 024001 (2001).
[6] D. G. Jenkins, C. J. Lister, M. P. Carpenter, P. Chowdhury, N. J. Hammond, R. V. F. Janssens, T. L. Khoo, T. Lauritsen, D. Seweryniak, T. Davinson, P. J. Woods, A. Jokinen, and H. Penttila, Phys. Rev. C **72**, 031303(R) (2005).
[7] J. Ekman, D. Rudolph, C. Fahlander, A. P. Zuker, M. A. Bentley, S. M. Lenzi, C. Andreoiu, M. Axiotis, G. de Angelis, E. Farnea, A. Gadea, Th. Kroll, N. Marginean, T. Martinez, M. N. Mineva, C. Rossi-Alvarez, and C. A. Ur, Phys. Rev. Lett. **92**, 132502 (2004).

[8] M. A. Bentley, C. Chandler, P. Bednarczyk, F. Brandolini, A. M. Bruce, D. Curien, O. Dorvaux, J. Ekman, E. Farnea, W. Gelletly, D. T. Joss, S. M. Lenzi, D. R. Napoli, J. Nyberg, C. D. O'Leary, S. J. Williams, and D. D. Warner, Phys. Rev. C **73**, 024304 (2006).
[9] M. A. Bentley, C. D. O'Leary, A. Poves, G. Martínez-Pinedo, D. E. Appelbe, R. A. Bark, D. M. Cullen, S. Erturk, and A. Maj, Phys. Lett. **B437**, 243 (1998).
[10] M. A. Bentley, C. D. O'Leary, A. Poves, G. Martínez-Pinedo, D. E. Appelbe, R. A. Bark, D. M. Cullen, S. Ertürk, and A. Maj, J. Phys. G **25**, 599 (1999).
[11] C. D. O'Leary, M. A. Bentley, D. E. Appelbe, D. M. Cullen, S. Ertürk, R. A. Bark, A. Maj, and T. Saitoh, Phys. Rev. Lett. **79**, 4349 (1997).
[12] J. Ekman, D. Rudolph, C. Fahlander, R. J. Charity, W. Reviol, D. G. Sarantites, V. Tomov, R. M. Clark, M. Cromaz, P. Fallon, A. O. Macchiavelli, M. Carpenter, and D. Seweryniak, Eur. Phys. J. A **9**, 13 (2000).
[13] M. A. Bentley, S. J. Williams, D. T. Joss, C. D. O'Leary, A. M. Bruce, J. A. Cameron, M. P. Carpenter, P. Fallon, L. Frankland, W. Gelletly, C. J. Lister, G. Martínez-Pinedo, A. Poves, P. H. Regan, P. Reiter, B. Rubio, J. Sanchez Solano, D. Seweryniak, C. E. Svensson, S. M. Vincent, and D. D. Warner, Phys. Rev. C **62**, 051303(R) (2000).
[14] J. Ekman, C. Andreoiu, C. Fahlander, M. N. Mineva, D. Rudolph, M. A. Bentley, S. J. Williams, R. J. Charity, E. Ideguchi, W. Reviol, D. G. Sarantites, V. Tomov, R. M. Clark,

M. Cromaz, P. Fallon, A. O. Macchiavelli, M. P. Carpenter, and D. Seweryniak, Phys. Rev. C **70**, 057305 (2004).

[15] S. J. Williams, M. A. Bentley, D. D. Warner, A. M. Bruce, J. A. Cameron, M. P. Carpenter, P. Fallon, L. Frankland, W. Gelletly, R. V. F. Janssens, D. T. Joss, C. D. O'Leary, C. J. Lister, A. Poves, P. H. Regan, P. Reiter, B. Rubio, D. Seweryniak, C. E. Svensson, and S. M. Vincent, Phys. Rev. C **68**, 011301(R) (2003).

[16] D. Rudolph, C. Baktash, M. J. Brinkman, M. Devlin, H.-Q. Jin, D. R. LaFosse, M. Leddy, I. Y. Lee, A. O. Macchiavelli, L. L. Riedinger, D. G. Sarantites, and C. H. Yu, Z. Phys. A **358**, 379 (1997).

[17] C. Andreoiu, M. Axiotis, G. de Angelis, J. Ekman, C. Fahlander, E. Farnea, A. Gadea, T. Kroll, S. M. Lenzi, N. Marginean, T. Martinez, M. N. Mineva, C. Rossi Alvarez, D. Rudolph, and C. A. Ur, Eur. Phys. J. A **15**, 459 (2002).

[18] L.-L. Andersson, E. K. Johansson, J. Ekman, D. Rudolph, R. du Rietz, C. Fahlander, C. J. Gross, P. A. Hausladen, D. C. Radford, and G. Hammond, Phys. Rev. C **71**, 011303(R) (2005).

[19] M. A. Bentley, C. Chandler, M. J. Taylor, J. R. Brown, M. P. Carpenter, C. Davids, J. Ekman, S. J. Freeman, P. E. Garrett, G. Hammond, R. V. F. Janssens, S. M. Lenzi, C. J. Lister, R. du Rietz, and D. Seweryniak, Phys. Rev. Lett. **97**, 132501 (2006).

[20] J. A. Nolan and J. P. Schiffer, Annu. Rev. Nucl. Sci. **19**, 471 (1969).

[21] A. J. Cox, J. M. G. Caraca, B. Schlenk, R. D. Gill, and H. J. Rose, Nucl. Phys. **A217**, 400 (1973).

[22] P. E. Garrett, W. E. Ormand, D. Appelbe, R. W. Bauer, J. A. Becker, L. A. Bernstein, J. A. Cameron, M. P. Carpenter, R. V. F. Janssens, C. J. Lister, D. Seweryniak, E. Tavukcu, and D. D. Warner, Phys. Rev. Lett. **87**, 132502 (2001).

[23] C. N. Davids *et al.*, Nucl. Instrum. Methods B **441**, 1224 (1989).

[24] I.-Y. Lee, Nucl. Phys. **A520**, 641c (1990).

[25] K. Shima, N. Kuno, and M. Yamanouchi, Phys. Rev. A **40**, 3557 (1989).

[26] E. Caurier, ANTOINE code, Strasbourg, 1989–2006.

[27] D. Bucurescu, C. A. Ur, S. M. Lenzi, D. R. Napoli, J. Sanchez-Solano, D. Bazzacco, F. Brandolini, G. de Angelis, E. Farnea, A. Gadea, S. Lunardi, N. Marginean, Zs. Podolyak, A. Poves, and C. Rossi Alvarez, Phys. Rev. C **67**, 034306 (2003).

[28] J. Duflo and A. P. Zuker, Phys. Rev. C **66**, 051304(R) (2002).

[29] E. K. Warburton and J. Weneser, in *Isospin in Nuclear Physics*, edited by D. H. Wilkinson (North Holland, Amsterdam, 1969), p. 175.